ERWIN L.HAHN
INSTITUTE
FOR
MAGNETIC
RESONANCE
IMAGING

ANNUAL REPORT

2017

Erwin L. Hahn Institute for Magnetic Resonance Imaging
Kokereiallee 7
45141 Essen
Germany

fon +49 (0) 201 1836070
fax +49 (0) 201 1836073
www.hahn-institute.de

Published by the Erwin L. Hahn Institute for Magnetic Resonance Imaging.

Preface

After the successful and positive evaluation of the Institute at the end of 2016, 2017 was a year of consolidation and planning for the long term. In particular, this involved a lengthy exploration with Siemens of the options for upgrading our current system. We will submit the application for an upgrade in 2018, and hope thereby to ensure our continued presence at the cutting edge of 7T research for the coming years.

A highlight of the year was the arrival of Peter Koopmans as an Emmy Noether laureate. Peter will build up a group looking at high spatial resolution functional (f)MRI and particularly layer-specific fMRI, using advanced acquisition techniques. During his time at the Institute he will enjoy the status of a PI.

On a sadder note, 2017 marked the departure of Corinna Heldt as our Administrative Director for bigger and better things as head of the Dean's office in the Electrical Engineering Faculty at the nearby University of Bochum. Corinna did a great job at the Erwin L. Hahn Institute, and we of course wish her every success in her new position. In autumn Judith Kösters arrived as her replacement, and we hope that she has both a successful and enjoyable time in this important position.

The Erwin L. Hahn lecture of 2017 was given by Christian Büchel of the University Medical Center Hamburg-Eppendorf, who gave an insightful lecture with the title "How expectation shapes pain: insights from brain and spinal cord imaging". This was the centrepiece of a day devoted to "Clinical Neuroimaging". This year the lecture was held in the Oktogon Building on the grounds of the "Zollverein", which lent a unique and pleasant atmosphere to proceedings. The entire meeting was well attended, and afterwards many compliments were paid both for the quality of the content and the organisation.

In the following short report of our activities you can see the full range of applications at 7T, from hardware development to applications of spectroscopy, and from imaging the brain to the prostate. You will also find some photos of the Erwin L. Hahn lecture. I hope that you find the content enjoyable and stimulating, and look forward to another year's exciting research at the Erwin L. Hahn Institute.

David Norris
Essen, January 2018

Parallel Transmit Capability of Various RF Transmit Elements and Arrays at 7T MRI

Remote radiofrequency (RF) body coils are generally implemented as built-in body coils for signal transmission in clinical MR systems at 1.5 and 3T. There, the transmit body coil is mounted on the bore liner of the MR system. Up to now, there is no remote body coil for body MRI at 7T. Instead, close-fitting transmit-receive coils have been used so far. With the MRexcite project at the Erwin L. Hahn Institute for MRI, pioneer research has been conducted in ultrahigh field body MRI by implementing a remote transmit/receive body coil [1,2] mounted on the bore liner.

A crucial step in the planning, construction, and validation of any coil array for ultrahigh field MRI is the performance of radiofrequency simulations. Since the behavior of complex geometries cannot be calculated analytically, the problem domain is separated into sub-volumes for which the Maxwell equations can be solved numerically. Using this approach, the problem can be simulated and the coil parameters can be optimized. Also, this procedure is mandatory for the assessment of the specific absorption rate (SAR) to guarantee the patient's safety.

In order to optimize the coil performance, we investigated different types of coil elements (Figure 1a-f). These elements were combined into four different configurations of circumferential RF body arrays with 4 or 8 transmit elements each and loaded with the body model DUKE [3] (Figure 1g-j). The gradient coil's shield was modeled as a perfect electric conductor and acts as an RF shield. After simulating these arrays in CST Microwave Studio (CST AG, Darmstadt, Germany), the coils were evaluated regarding metrics such as coupling behavior, power balance, degrees of freedom (DOF) offered by the individual transmit patterns [4], and power as well as SAR efficiency using virtual observation points [5].

It could be shown that independent of the coil element type, arrays with 4 elements are intrinsically well decoupled (below -20 dB). In comparison, arrays with 8 elements show comparably high inter-element coupling (maximum values of about -10 dB) compared to close-fitting coil arrays. This can be attributed to the reduced distance between the elements and the low coupling to the subject tissue. Note that no additional decoupling networks were employed.

For the two investigated shim settings (circularly polarized and phase-only shim optimized for a kidney-sized region in the body center), up to 30% of the power is dissipated in the bore liner. The rest is dissipated in the lumped elements, capacitors in the tuning and matching network, radiated, or absorbed in the body model. Even though the losses are quite unevenly distributed, the power going into the body model is quite similar in all cases – between 40% and 60%.

The DOFs offered by the transmit patterns was evaluated using a singular value decomposition for central slices in 3 orthogonal orientations. It could be shown that the encoding capabilities for all arrays are maximum in the transversal orientation, followed by the coronal and sagittal orientation. Furthermore, it could be shown that in general no 4-element array is able to achieve performance equal to the worst 8-channel array.

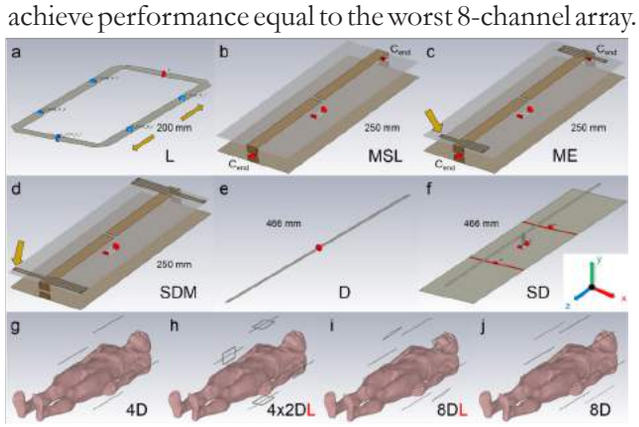

Figure 1: Depiction of the 6 investigated coil elements (a-f): rectangular loop (a), microstrip line (MSL) (b), meander element (ME) obtained by introducing meander structures (arrow) at the end of the microstrip line (c), shielded dipole with larger (arrow) meanders (SDM) and without end capacitors (d), lambda-over-two dipole (e), and shielded (SD) lambda-over-two dipole (f). The four investigated array topologies (g-j) with 4 identical elements (g), a hybrid of 4 loops and 4 other elements of one type where elements of different types are located at the same position (h), a hybrid of 4 elements of one type combined with 4 loops in between (i), and 8 identical elements (j) combined on a circumferential ring. Here, the scheme is shown for dipoles.

Stefan H.G. Rietsch, Stephan Orzada, Andreas K. Bitz, Marcel Gratz, Mark E. Ladd, Harald H. Quick

Investigations of the power efficiency were accomplished on a voxelwise basis. This means that for the central slices in transversal, coronal, and sagittal orientation, the maximum achievable B_1^+ amplitude for each voxel on an isotropic 128x128 grid was calculated by summing the absolute values of the B_1^+ of each RF channel. The comparison shows that in general 8SD perform best in most regions and especially in the center of the subjects (closely followed by 8D). With a realistic power budget of 8 kW, up to 25 µT can be achieved in the border regions, while in the center of the body model values of 10 µT are possible. Compared to values from recent literature, remote coils suffer from reduced power efficiency in comparison to close-fitting coils.

As for the power efficiency, the SAR efficiency was evaluated on a voxelwise basis. In Matlab, 60 RF shims were calculated (2x Intel Xeon X5690, 12 cores in total) for each voxel in the central slices using non-linear optimization (Nelder-Mead simplex search method) with arbitrary starting points in order to maximize the SAR efficiency ($B_1^+ \bullet \max(SAR_{10g})^{-0.5}$). The results are shown in Figure 2. For 8D the SAR efficiency drops heavily towards the center in transversal orientation (Figure 2a) compared to the other orientations (Figure 2b,c). This seems reasonable since high B_1^+ in the center might go along with high local SAR values in the outer regions. In Figure 2d-f the performance among the arrays is compared. In most of the areas of the central transversal slice (Figure 2d), 8SD and 8D achieve the maximum voxelwise SAR efficiency. This is especially important in the center of the body where deep-lying organs and structures of clinical interest are located. The arrays 8SD and 8D also show the best performance throughout large regions in the coronal and sagittal planes, which may be explained by the geometrical length. Toward the border regions in z-direction, RF arrays with MSL elements perform best. Figure 2g-i indicate quantitatively how much more SAR-efficient 8SD are in comparison to the next-best array, with 8D being excluded. This makes sense since 8D and 8SD perform very similarly in the context of this investigation. On average, 8SD are only 0.35% more SAR efficient than 8D in this voxelwise comparison. In the transversal orientation, 8SD on average perform 7.7% better than the next-best array (excluding 8D), in the sagittal orientation this value is 7.1%, and in the coronal orientation it is 15.6%. Comparing the best and the worst array (8D included) yields an average factor of 3.04 (max/min) in the transversal, 4.07 in the sagittal, and 4.05 in the coronal orientation.

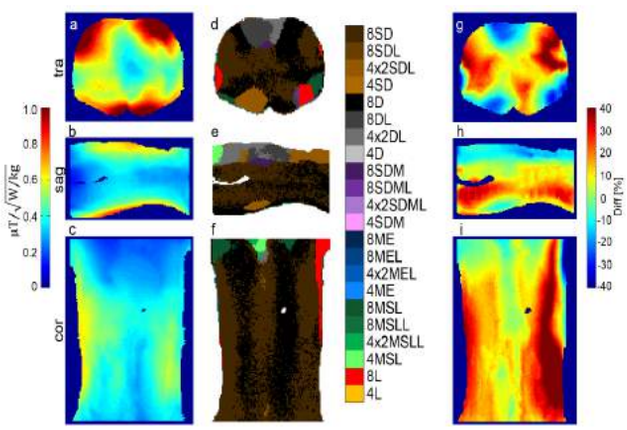

Figure 2: Results of the voxelwise SAR efficiency for 8 dipoles (a-c) in the body model. Each pixel in the central transversal (a), sagittal (b), and coronal (c) planes represents one shim with optimized SAR efficiency for this pixel. As can be seen, the SAR efficiency is lower in the center of the body model (a). If all arrays are compared (d-f), 8D and 8SD show the highest SAR efficiency in most of the areas, especially in the center of the body model. (g-i) show by how much 8SD outperform the second-best array (excluding 8D) if 8SD are the best performing array (positive values) or by how much 8SD underperform the best array (negative values). Scales in all figures are cropped.

The results indicate that 8 SD are most power and SAR efficient in the context of the investigations. Furthermore, the evaluation of the cumulative sum of singular values showed that this configuration features high encoding capability. In the absence of additional decoupling methods, coupling was found to be an issue for all arrays with 8 elements; thus, investigations of decoupling strategies could be a field of further research. As part of the MRexcite project, a remote body coil with 32 ME elements mounted on the bore liner has been implemented at 7T. ME elements were chosen rather than SD or D because of their more compact size in the z-direction.

References: [1] Orzada S. et al. ISMRM 2015. #630; [2] Orzada S. et al. ISMRM 2016. #167; [3] Christ A. et al. Phys Med Biol 2010;55(2):N23–38; [4] Eichfelder G., Gebhardt M. Magn Reson Med 2011;66(5):1468–76; [5] Guérin B. et al. Magn Reson Med 2014;73:1137–50

The research leading to these results has received funding from the European Research Council under the European Union's Seventh Framework Programme (FP/2007-2013) / ERC Grant Agreement n. 291903 MRexcite. The content is based on the original publication in Magnetic Resonance in Medicine: Rietsch et al. - Parallel Transmit Capability of Various RF Transmit Elements and Arrays at 7T MRI (DOI 10.1002/mrm.26704).

The German Ultrahigh Field Imaging (GUFI) Project – Update on past and recent activities

The GUFI network is a user group of 13 German and neighboring sites that all operate UHF (7T or 9.4T) MRI systems (Figure 1). The GUFI network was founded at the end of 2013 with the aid of DFG funding provided by the call to establish Core Facilities including distributed national networks. The initial project duration of three years (2013-2016) [1] was prolonged for another 36-month period (2016-2019) [2]. The overall goal of GUFI is to facilitate and harmonize the work of the German UHF sites.

In the past three and a half years, GUFI has made important contributions to address challenges for all German UHF sites and identify several new areas of common interest. A web-based platform has been established to inform external users about the technical and methodological possibilities at each of the UHF MR sites in Germany (www.mr-gufi.de). The website acts as a central point of contact for external scientists, giving explicit contact information for their desired site, and it is used to inform about and promote the research activities at UHF.

Figure 1: Sites of the GUFI network. All sites are operating UHF (10x 7T, 2x 9.4T) MRI systems provided by the same vendor (Siemens Healthcare). While most hardware components and the software/image processing are similar, there are different device generations and platforms within the GUFI network with differences regarding the magnets, the gradient coils and the RF head coils.

To harmonize access procedures between sites and thereby to facilitate access to UHF systems for external researchers, a consensus guideline document has been formulated that gives basic recommendations regarding access procedures and rules [3]. Furthermore, the GUFI partners defined and signed a consensus recommendation for dealing with subjects with passive implants [4], including a flowchart with decision boxes to standardize decision-making regarding whether a measurement at UHF MRI can be performed safely.

Quality assurance (QA) has also emerged as a critical issue for UHF systems and a topic of common interest to all GUFI members, as there are as yet no commonly accepted standards that adapt QA procedures at lower field strengths to the special needs at UHF. GUFI has implemented a QA protocol to assess coil and system performance based on SNR, B_1^+, noise, and stability measures. This protocol was initially used to compare QA parameters between all GUFI sites with the available on-site equipment. Very good agreement was found between the sites, but the protocol also revealed hardware and calibration faults at some sites; the underlying issues could be identified and rectified by the vendor based on the problem description delivered by the data, and repeat measurement verified conformance of the systems with desired specifications.

These measurements also demonstrated the need for a common QA phantom with realistic properties to compare inter-site data. Great effort has been spent as part of the GUFI project to compare different phantom materials and develop a phantom that emulates the dielectric properties and the relaxation behavior of brain tissue at 7T, making the phantom realistic and appropriate for QA purposes. A prototype version of this GUFI QA phantom (Figure 2) has already been tested at four sites and proven suitable for QA [5] (Fig 3). A revised version of this phantom in which the housing and recipe have been slightly modified to be more stable and to emulate the coil load of an human head even better has been built and calibrated

at one site, and is ready to be shipped to all GUFI partners.

For the special needs of the parallel RF transmission (pTx) systems used at UHF, an image-based QA procedure has been developed and tested with different setups at a few sites [6]. This method has proved to be reliable in detecting specific hardware deficiencies as well as assessing the reproducibility of pTx excitation patterns across different sites [7]. The excellent agreement between sites found in phantom measurements encouraged the GUFI participants to compare system reproducibility in human subjects.

Figure 2: Prototype of the GUFI phantom used for testing of the QA protocol at four GUFI sites. The head and neck part of the phantom is filled with a PVP water solution doped with NaCl and gelled with Agar. This resulted in realistic dielectric properties compared to the emulated tissue (ε_r =55, C=0.6 S/m) with proper T2 (60 ms) and acceptable T1 (700 ms) relaxation time constant. The shoulder part is filled with a NaCl-doped PVP solution to simulate the dielectric coil load of the human shoulder and body.

This study, targeted toward validating multicenter brain imaging at 7T, became known as the "traveling heads" study [8], since the same two subjects were imaged at eight 7T sites of the GUFI network with the identical imaging protocol. High reproducibility was found at all sites, but differences in inter-site versus intra-site reproducibility were identified that could be correlated to hardware differences between the individual sites, in particular the version of the RF head coil available.

The next important milestones within the GUFI project are: finalize a guidance document regarding the safety testing of RF coils built in-house, programming of an online tool for common safety instruction of UHF laboratory users, establishment of a platform to exchange information like imaging protocols or safety information regarding specific imaging devices and implants and, finally, refinement of automated analysis of pooled QA data. The German UHF MR community was the first national UHF MR community to coordinate their efforts in a network such as GUFI, and the high visibility of this project is demonstrated by the active involvement of international UHF MR sites and the establishment of a UK UHF MR network (UK7T) based on a similar concept, with which GUFI closely cooperates.

Figure 3: Inter-site and long-term analysis of the QA data. Second and third EPI time series (same-colored lines in the plots) are shown to compare the UHF MRI systems in a defined warm-up state. Site 1 had a system malfunction during the measurements on 2016/10/28 (red ellipse) with unusually high signal fluctuations. Restarting the system solved the problem. (May have been caused by loose RF coil contacts or timing error of hardware components.). Phantom #1 at Site 1 became leaky due to an accident in October 2016. The phantom was replaced resulting e.g. in different Signal-to-fluctuation-noise ratio level at Site 1 (brown ellipse).

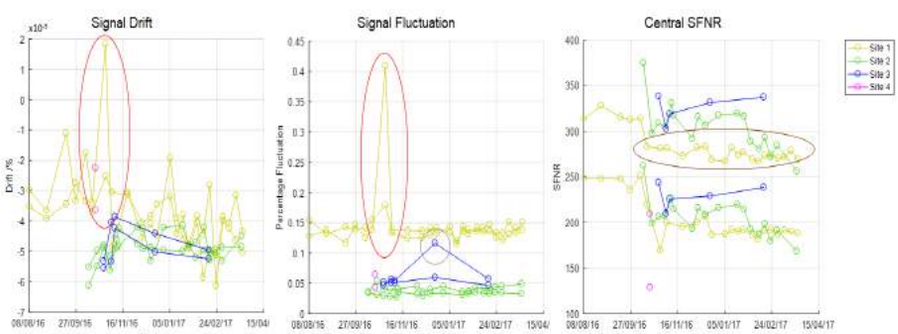

References: [1] German Research Foundation (DFG), DFG-Kennzeichen LA 1325/5-1; "German Ultrahigh Field Imaging (GUFI)"; PIs: Mark E. Ladd, Oliver Speck, David G. Norris; funding: 450000€; duration 36 months (start: 10/2013); [2] German Research Foundation (DFG), DFG-Kennzeichen LA 1325/7-1, QU 154/5-1; "German Ultrahigh Field Imaging (GUFI); PIs: Mark Ladd, Oliver Speck, Harald Quick; funding: 355000€, duration 36 months (start: 03/2017), [3] GUFI. Recommendations regarding access procedures and user access rules at German ultrahigh- field sites. http://www.mr-gufi.de/en/documents: 2016. [4] GUFI. Approval of subjects for measurements at ultra-high-field MRI. http://www.mr-gufi.de/en/documents: 2016. [5] Voelker MN, Kraff O, Pracht E, Wollrab A, Bitz AK, Stöcker T, Quick HH, Speck O, Ladd ME. Quality Assurance Phantoms and Procedures for UHF MRI - The German Ultrahigh Field Imaging (GUFI) Approach. 2017; Honolulu. Proc. of the International Society for Magnetic Resonance in Medicine. p 3912. [6] Gratz M, Völker M, Johst S, Ladd ME, Quick HH. Semi-automatic quantification of long-term stability and image quality of a parallel transmit system at 7T. 2015; Toronto. Proc. of the International Society for Magnetic Resonance in Medicine. p 2495. [7] Voelker MN, Brenner D, Flöser M, Gratz M, Johst S, Orzada S, Stöcker T, Quick HH, Ladd ME, Kraff O. On the robustness and reproducibility of spatially selective excitation using parallel transmission at 7T – a multicenter study. 2016; Singapore. Proc. of the International Society for Magnetic Resonance in Medicine. p 354. [8] Voelker MN, Kraff O, Brenner D, Wollrab A, Weinberger O, Berger MC, Robinson S, Bogner W, Wiggins C, Trampel R, Stöcker T, Niendorf T, Quick HH, Norris DG, Ladd ME, Speck O. The traveling heads: multicenter brain imaging at 7 Tesla. MAGMA 2016: doi: 10.1007/s10334-016-0541-8.

Cognitive Neuroscience and Behavioral Addictions

The research group investigates neural correlates of cognitive and emotive processes by using functional magnetic resonance imaging (fMRI). The main focus is on decision-making abilities and the intervening effects of executive control and emotional processes. One important clinical application of the basic research on cognitive and emotive interactions is the field of behavioral addictions. In the past, we have published studies on cue-reactivity and craving in the context of an uncontrolled and excessive use of Internet pornography (Brand et al., 2016). Characteristic for our research is the development and testing of different experimental paradigms in behavioral settings and the transfer to fMRI research for both basic research and clinical investigations.

One example of our current interests in the field of human-computer interaction is decision-making in the context of social media use. One recent project examines the decision-making processes involved when selecting a specific physician on the basis of information and recommendations available on social media sites. Previous behavioral studies demonstrated that participants with low executive functioning make decisions, which were based on subjective features of social media recommendations (such as the comments and ratings provided by other users), whereas high executive functioning participants prefer objective features. The recent project designed a decision-making task for fMRI research to investigate the neural correlates of decision-making performance in the social media context. Another project in the field investigates the cognitive and emotional neural correlates with respect to selfie postings of one's self vs. others in the context of Facebook. These studies should help to understand how users make decisions with different social media tools and what is the neural basis for this.

Another research area focusses on the neurobiological and neuropsychological characteristics of behavioral addictions, such as Internet-use disorders or pathological buying. Primarily, brain responses to addiction-related stimuli and their relevance for subjective desire are examined, as mentioned above with respect to Internet-pornography-use disorder.

More recently, the interaction effects between executive prefrontal performance and limbic-emotive processes are of interest. For this reason, neural correlates of inhibition performance against visual pornographic stimuli are currently being investigated in the context of Internet pornography-use disorder. It is supposed that there is a relationship between the tendency towards pathological use of Internet

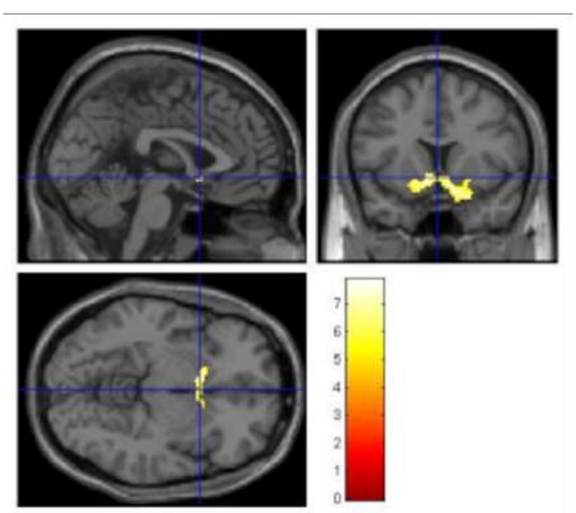

shopping cues > control cues

Contrast	Nearest brain region	Lat.	k	MNI - Coordinates x	y	z	*t*	*p*
Path. buyer	Striatum	L	370	-8	10	-10	7.78	< .001
		R		10	10	-12	7.79	< .001
		R		20	10	-10	5.92	< .001
	Parietal cortex (BA 5)	R	107	26	-44	72	7.44	< .001
	Anterior PFC (BA 10)	R	57	6	58	22	5.67	< .001
Control participant	Non significant activation							

FWE corr., p < .05, k = 10)

Figure 1: *Right:* Preliminary results of one pathological buyer and one age and gender matched control participant in the shopping cue > control cue contrast. Left: Activations within the striatum in the patient with pathological buying in the contrast shopping cue > control cue.

pornography and the neural correlates of inhibitory control and craving reactions as shown on a behavioral level (Antons & Brand, 2018). Therefore, a stop-signal paradigm has been modified for fMRI research to allow the assessment of executive inhibition performance, not only in the context of Internet pornography-use disorder, but also in various other behavioral addictions. One further study investigates cue-reactivity and craving in the context of pathological buying. It is supposed that cue elicited craving reactions are one of the main mechanisms for the dysfunctional, excessive buying behavior (Trotzke et al., 2014). Neural correlates for cue-induced craving had never been investigated in this clinical condition, so far. A modified version of the cue-reactivity paradigm with shopping pictures that had been used in the context of Internet pornography-use disorder (Brand et al., 2016) has been developed and applied to patients who suffer from pathological buying and healthy control participants. The project is funded by the DFG. Preliminary results on single-case level, for example, demonstrate a higher activation in the (ventral) striatum, the parietal cortex and the anterior prefrontal cortex for the patient with pathological buying behavior in the contrast shopping cue > control cue. The control participant, however, does not exhibit such activations in the same contrast condition (see Figure 1).

References: [1] Antons, S. & Brand, M. (2018). Trait and state impulsivity in males with tendency towards Internet-pornography-use disorder. Addictive Behaviors., 79, 171-177. doi:10.1016/j.addbeh.2017.12.029 [2] Brand, M., Snagowski, J., Laier, C., & Maderwald, S. (2016). Ventral striatum activity when watching preferred pornographic pictures is correlated with symptoms of Internet pornography addiction. Neuroimage, 129, 224-232. doi:10.1016/j.neuroimage.2016.01.033 [3] Trotzke, P., Starcke, K., Pedersen, A., & Brand, M. (2014). Cue-induced craving in pathological buying: Empirical evidence and clinical implications. Psychosomatic Medicine, 76, 694-700.

Cerebellar fMRI – Modulated cerebellar activation during acquisition, extinction and reacquisition of conditioned eyeblink responses

The research group of Professor Timmann focuses on the involvement of the cerebellum in a range of different forms of motor learning. Functional (f)MRI is the method of choice to map behavioral patterns to the test subject's anatomy. At 7T, the superior signal-to-noise ratio does allow inferences not only on the level of the superficial cerebellar cortex but also on the level of deep cerebellar structures, the cerebellar nuclei, which play a critical role in the cerebellar function.

Classical delay eyeblink conditioning is likely the most commonly used paradigm to study cerebellar learning. In eyeblink conditioning an air puff (unconditioned stimulus) is administered to the eye shortly after a preceding tone (conditioned stimulus) was played. This gradually leads to a timed eyeblink response initiated after hearing the conditioned stimulus (conditioned eyeblink response). As yet, few studies have focused on extinction and savings of conditioned eyeblink responses. The term extinction describes the gradual inhibition of conditioned behavior when it is no longer needed. Saving effects, which are reflected in a reacquisition after extinction that is faster than the initial acquisition, suggest that learned associations are at least partly preserved during extinction.

In a 7T study, Prof. Timmann's group recently tested the hypothesis that acquisition-related plasticity is anihilated during extinction in the cerebellar cortex, but retained in the cerebellar nuclei, allowing for faster reacquisition. Changes of 7T fMRI signals were investigated in the cerebellar cortex and nuclei of young and healthy human subjects. Main effects of acquisition, extinction, and reacquisition against rest were calculated in conditioned stimulus-only trials. Individual (first-level) activations (β-values) were determined for a spherical region of interest (ROI) around the acquisition peak voxel in lobule VI, and dentate and interposed nuclei ipsilateral to the unconditioned stimulus. In the cerebellar cortex and nuclei, fMRI signals were significantly lower in extinction compared to acquisition and reacquisition, but not significantly different between acquisition and reacquisition. These findings are consistent with the theory of bidirectional learning in both the cerebellar cortex and nuclei. It cannot explain, however, why conditioned responses reappear almost immediately in reacquisition following extinction. Although the present data do not exclude that part of the initial memory remains in the cerebellum in extinction, future studies should also explore changes in extra-cerebellar regions as a potential substrate of saving effects.

References: [1] Ernst, T. M., Thürling, M., Müller, S., Kahl, F., Maderwald, S., Schlamann, M., Boele, H. J., Koekkoek, S. K. E., Diedrichsen, J., De Zeeuw, C. I., Ladd, M. E., & Timmann, D. (2017). Modulation of 7 T fMRI signal in the cerebellar cortex and nuclei during acquisition, extinction, and reacquisition of conditioned eyeblink responses. Human Brain Mapping, 38, 3957-3974.

Research Funded by the German Research Foundation, DFG TI 239/10-1, 10-2.

Thomas M. Ernst, Markus Thürling, Stefan Maderwald, Mark E. Ladd, Dagmar Timmann

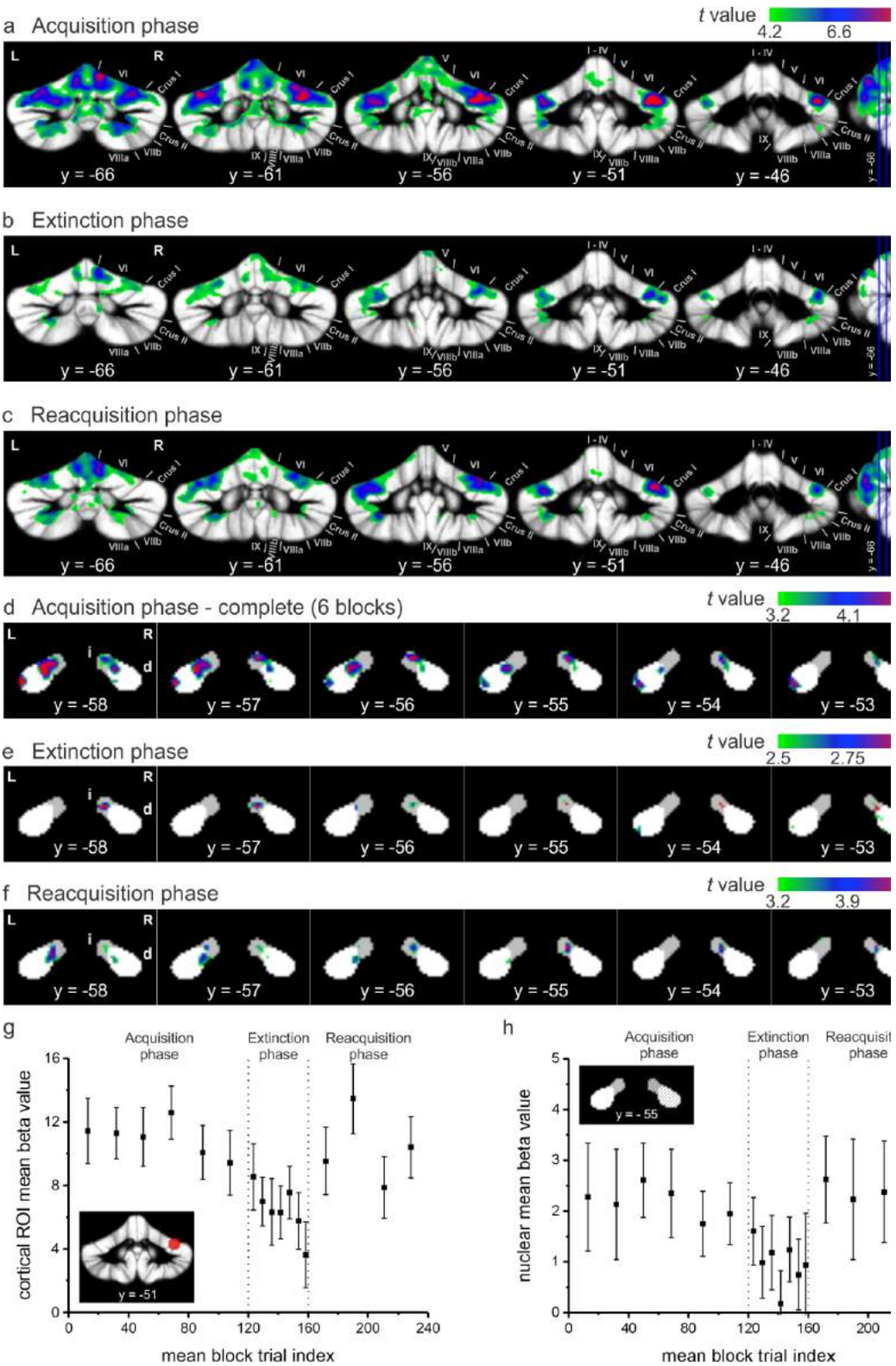

Figure 1: Activation patterns and mean region-of-interest (ROI) β values in the cerebellar cortex (a-c,g) and the deep cerebellar nuclei (d-f,h) during all phases (acquisition, extinction, reacquisition) of the behavioral eyeblink conditioning experiment.

USPIO-enhanced MRI for the detection of lymph node metastases

Feasibility of USPIO-enhanced MRI for detecting lymph node metastases in prostate cancer on 7 Tesla

Lymph nodes often are the first station of metastasis in prostate cancer and it is important to detect them at an early stage. Ultrasmall superparamagnetic iron oxide (USPIO) enhanced MRI is a technique to diagnose pelvic lymph node metastases [1,2]. The particles accumulate in healthy lymph node tissue, resulting in significant signal loss on strongly T2*-weighted (T2*W) imaging. Parts of the lymph node that contain metastases from prostate cancer do not accumulate USPIOs and will therefore retain MR signal intensity. By performing USPIO-enhanced MRI on a higher field strength, signal-to-nose and therefore resolution can be improved. In addition, the susceptibility effect of USPIOs becomes stronger on higher field strengths. This offers opportunities, because it might allow the detection of smaller lymph nodes metastases and improve the differentiation between healthy lymph nodes and metastases. Here we show the feasibility of USPIO-enhanced MRI for detecting pelvic lymph node metastases of prostate cancer on our 7 Tesla MRI system.

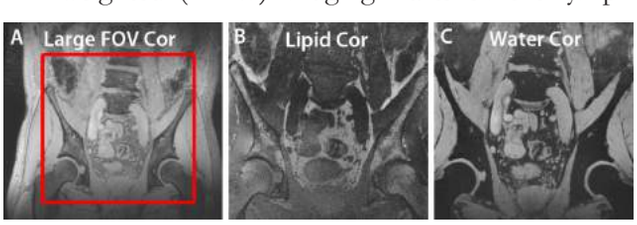

Figure 1: An overview coronal (A), lipid-selective coronal (B) and water-selective (computed TE= 8 ms) coronal image (C) of a patient with prostate cancer. The red box indicates the FOV of the lipid- and water-selective images. The overview image featured a FOV of 384x384x192 mm3 and voxelsize of 1x1x1 mm3.

Patients with high risk prostate cancer were scanned 24-36 hours after a USPIO (ferumoxtran-10) dose of 2.6 mg iron per kg of bodyweight, which was dissolved in 100cc saline and administered intravenously over a period of 30-45 minutes. In addition, they received an intramuscular dose of scopolamine butylbromide just before the MRI scan. On our 7T system we used the 8 channel ^{1}H transceiver body-array coil with meander-type microstrip elements [3]. After B_0 and B_1^+ shimming, water and lipid selective imaging was performed using the TIAMO [4] technique to obtain homogeneous body imaging. The scanned area contained at least the area from the aorta bifurcation to the base of the bladder.

Lipid selective imaging was performed with a 3D gradient echo (GRE) sequence with a TE of 2.09 ms, TR of 5.2 ms, voxel size of 0.66x0.66x0.66 mm^3 (FOV 210x210x169 mm^3, matrix 320x320x256) and acquisition time of 2 minutes and 51 seconds. Water-selective imaging was performed using a 3D multi-GRE sequence with a 970 µs water selective block pulse, TR of 14 ms, voxel size of 0.66x0.66x0.66 mm^3 (FOV 210x210x169 mm^3, matrix 320x320x256), acquisition

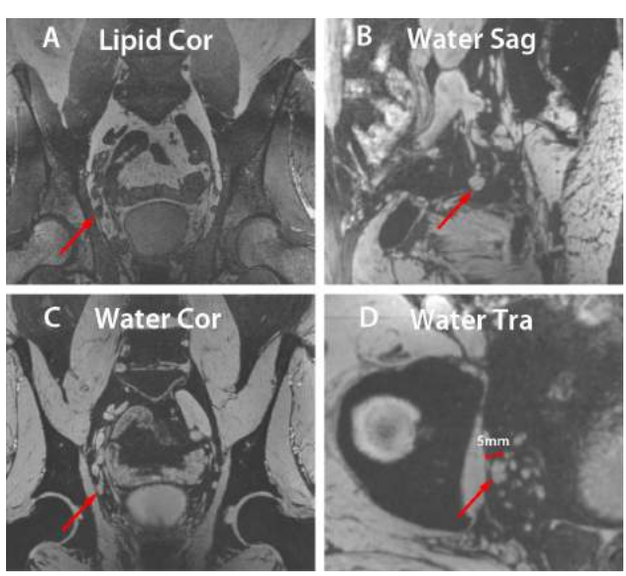

Figure 2: A lymph node (red arrow) is indicated on the lipid- and water selective (computed TE = 8ms) coronal images (A,C) in a patient with prostate cancer recurrence after radiotherapy. The lymph node is depicted on a zoomed sagital (B) and transversal image (D) as well, with an indication of the short axis dimension of the node on the transversal image. The lymph node does not appear to take up USPIO contrast on iron-sensitive water-selective imaging and shows an irregular shape, making it highly suspicious to be metastatic.

time of 8 minutes and 23 seconds and multiple T2* weighted contrasts (TE of 2.10, 4.19, 6.21, 8.30 and 10.32 ms), from which computed TE images were reconstructed using a weighted linear least squares fitting procedure [5,6].

The lipid- and water selective T2*W images feature a high spatial resolution and separate lipid and water signals well (Figure 1). The lipid-selective sequence allows the detection of normal USPIO rich lymph nodes, due to the bright lipid background. The high resolution water-selective imaging allows lymph nodes to be assessed on shape and size in three different orientations (Figure 2).

The computed echo time imaging enables the choice of echo time with accompanying T2* weight and can be used to separate lymph nodes with and without USPIO uptake. Particularly, the extrapolated TE=18ms image shows a completely black image for a lymph node with USPIO uptake, whereas the suspicious lymph node still appears bright on the same image set. This is also reflected by the R2* map (Figure 3).

Our results show that imaging of the pelvis on 7 Tesla MRI is feasible at a high spatial resolution and enables an accurate evaluation of lymph node size and shape. In addition, it may allow the detection of very small lymph node metastases. The susceptibility of USPIO particles results in large R2* values on ultrahigh field. Computed TE imaging, including the R2* map, provides the tools to optimize TE and to quantitatively assess USPIO uptake, such that differentiation between normal lymph nodes and metastases can be optimized. Additional clinical studies need to be performed to assess how these technical advances translate to clinic.

In summary, we showed that USPIO enhanced MRI for detecting lymph node metastases in prostate cancer on 7 Tesla is feasible and allows computed echo time imaging at a high spatial resolution.

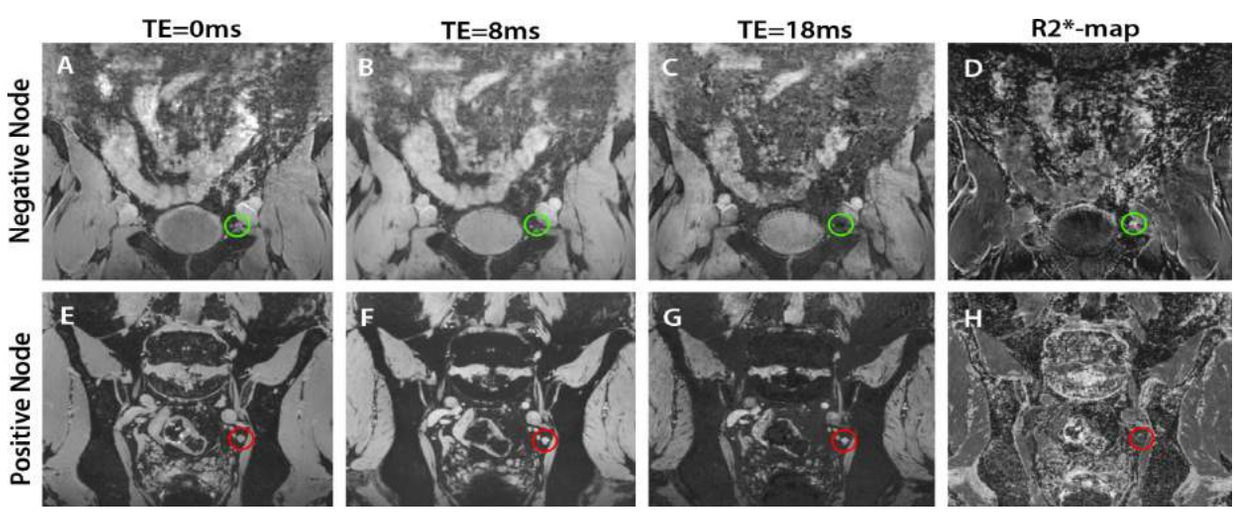

Figure 3: water-selective T2*W images of a lymph node suspect for metastasis (E,F,G) and a normal lymph node (A,B,C) at different computed echo times. In addition an R2*-map is shown of these lymph nodes (D,H). The normal lymph node takes up USPIOs and therefore appears dark on strongly T2*W imaging and has a high value on the R2* map. The metastatic lymph node has no substantial USPIO uptake and therefore features no appreciable T2* weighting and has a low value on the R2* map.

References: [1] Heesakkers RA, Jager GJ, Hovels AM, de Hoop B, van den Bosch HC, Raat F, Witjes JA, Mulders PF, van der Kaa CH, Barentsz JO. Prostate cancer: detection of lymph node metastases outside the routine surgical area with ferumoxtran-10-enhanced MR imaging. Radiology 2009;251(2):408-414. [2] Harisinghani MG, Barentsz J, Hahn PF, Deserno WM, Tabatabaei S, van de Kaa CH, de la Rosette J, Weissleder R. Noninvasive detection of clinically occult lymph-node metastases in prostate cancer. N Engl J Med 2003;348(25):2491-2499. [3] Orzada S, Quick HH, Ladd ME, Bahr A, Bolz T, Yazdanbakhsh P, Solbach K, Bitz AK. A flexible 8-channel transmit/receive body coil for 7 T human imaging 2009; Honolulu, Hawaii, USA. p 2999. [4] Orzada S, Maderwald S, Poser BA, Bitz AK, Quick HH, Ladd ME. RF excitation using time interleaved acquisition of modes (TIAMO) to address B1 inhomogeneity in high-field MRI. Magn Reson Med 2010;64(2):327-333. [5] Philips BWJ, Fortuin AS, Orzada S, Scheenen TWJ, Maas MC. High resolution MR imaging of pelvic lymph nodes at 7 Tesla. Magn Reson Med 2017;78(3):1020-1028. [6] Veraart J, Sijbers J, Sunaert S, Leemans A, Jeurissen B. Weighted linear least squares estimation of diffusion MRI parameters: strengths, limitations, and pitfalls. Neuroimage 2013;81:335-346.

Enhanced GABA concentration in the medial prefrontal cortex of type 2 diabetes patients is associated with episodic memory dysfunction

Over recent years there has been an upsurge in interest in 1H- Magnetic Resonance Spectroscopy (MRS) as a non-invasive method to quantify GABA and glutamate concentrations in specific regions of the human brain. GABA and glutamate are respectively the main inhibitory and excitatory neurotransmitter in the brain and are essential in cognitive processes as for instance memory. We previously showed (Thielen et al, in press) that medial-prefrontal (mPFC) glutamate/glutamine but not GABA levels increased during an episodic memory task, which appeared to be positively related to memory performance. With respect to GABA, Floyer-Lea and colleagues (2006) demonstrated that motor sequence learning reduced the GABA concentration within the sensorimotor cortex. This reduction was specific to motor learning since an unlearnable, non-repetitive motor sequence did not reduce GABA concentration in the sensorimotor cortex. These studies are important since they showed that MRS is sensitive to memory related neurotransmitter concentration changes which "mirror" pharmacological studies showing memory decrease/increase due to the administration of GABA/glutamate agonists. Since, human pharmacological studies cannot probe the properties of GABA/glutamate in isolated brain regions MRS provide a powerful tool to assess GABA/glutamate in specific brain networks.

Type 2 diabetes (T2D) patients suffer from impairment in a variety of cognitive domains. Among these impairments, the most robust and frequently reported cognitive deficits in T2D are those that relate to episodic memory (Jones et al., 2014) and there is strong evidence supporting a relation between T2D and neurocognitove disorders and Alzheimers disease in particular (Ott et al., 1999; Leibson et al., 1997).

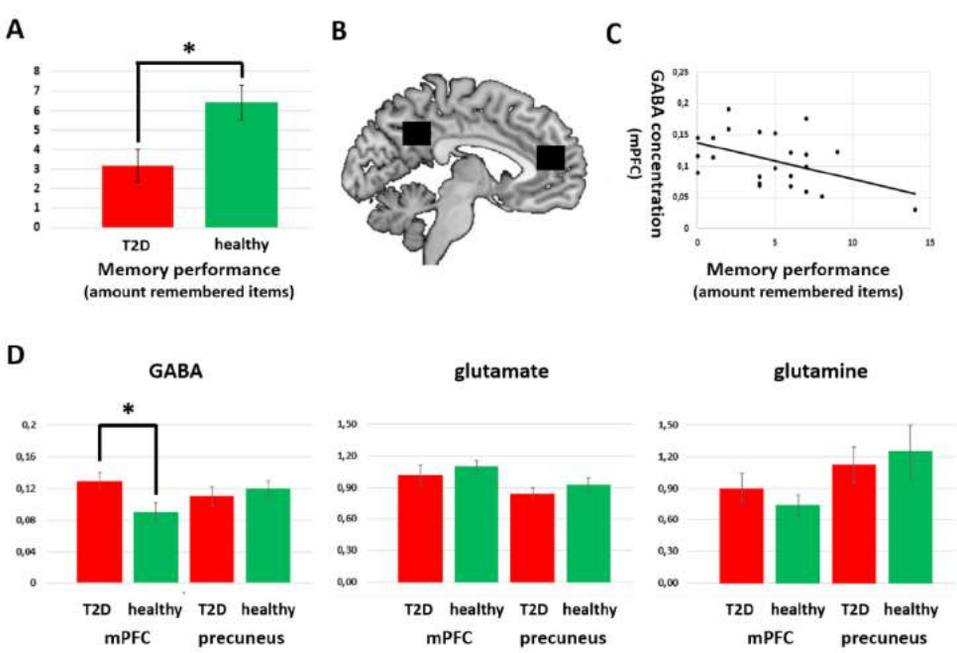

Figure 1: A) The decreased memory performance of type 2 diabetic (T2D) patients. B) The positions of the MRS voxels (black squares) are depicted. The right (anterior) voxel is located in the mPFC whereas the left (posterior) voxel is located in the precuneus. C) Correlation between mPFC GABA/NAA ratio and memory performance across all subjects. D) The mean concentrations of GABA (left), glutamate (middle) and glutamine (right) in the mPFC and precuneus of type 2 diabetic (T2D) patients (red) and healthy control subjects (green). Only the GABA/NAA ratio in the mPFC appeared to be significant different between the groups.

Jan-Willem Thielen, Donghyun Hong, Seyedmorteza Rohani Rankouhi, Bixia Chen, Michael Roden, David G. Norris, Indira Tendolkar

The pathophysiological mechanisms of T2D related cognitive dysfunction are not entirely understood. In rodent, it has been shown that T2D is associated with a malfunctioning homeostasis of GABA and glutamate (Sickmann et al., 2010). By utilizing MRS at a 1.5 Tesla scanner, Sinha and colleagues (2014) found an increased glutamate+glutamine (GLx) concentration in the right frontal region of T2D patients. Unfortunately, whether this effect was related to glutamate, glutamine or both could not be elucidated since it is difficult to sepa-rate glutamate from glutamine at lower magnetic field strengths (Moser et al., 2012). In addition, Bussel and col-leagues (2016) found an increased GABA concentration in the occipital lobe of T2D patients that was related to lower cognitive performance. However, the occipital lobe is thought to be a visual processing area that is not primary involved in the control of higher cognitive functions as episodic memory. Therefore, we utilized MRS at ultra-high magnetic field strength (7 Tesla) to investigate T2D related changes of amino acid concentrations in episodic memory specific regions. Since the medial prefrontal cortex (mPFC) and precuneus exhibit increased episodic memory related brain activation (fMRI) in healthy elderly (Thielen et al., 2016) we measured GABA, glu-tamate and glutamine concentrations in these areas and related these concentrations to episodic memory performance and T2D. We found that T2D patients had a decreased memory for face-profession associations and an elevated GABA concentration in the mPFC but not precuneus (figure 1). Moreover, mPFC GABA concer-tation, across all subjects, was negatively associated with memory performance suggesting that abnormal GABA levels in the mPFC is linked to the episodic memory deficit occurring in T2D patients. Since lifestyle factors, such as regular physical activities have been shown to counteract memory decline in healthy elderly, we are currently assessing whether an exercise intervention improves episodic memory in T2D and whether this is associated with a normalization of the mPFC GABA concentration.

References: [1] van Bussel FC, Backes WH, Hofman PA, Puts NA, Edden RA, van Boxtel MP, et al. (2017) : Increased GABA concentrations in type 2 diabetes mellitus are related to lower cognitive functioning. Medicine (Baltimore). doi:10.1097/MD.0000000000004803. [2] Floyer-Lea A, Wylezinska M, Kincses T, Matthews PM (2006) Rapid modulation of GABA concentration in human sensorimotor cortex during motor learning. J Neurophysiol.,95: 1639-44. [3] Leibson CL, Rocca WA, Hanson VA, Cha R, Kokmen E, O'Brien et al. (1997) Risk of dementia among persons with diabetes mellitus: a population-based cohort study. Am J Epidemiol., 145: 301–308. [4] Moser E, Stahlberg F, Ladd ME, Trattnig S (2012) 7-T MR--from research to clinical applications? NMR Biomed., 25: 695-716. [5] Ott A, Stolk RP, Van Harskamp F, Pols HA, Hofman, A, Breteler MM (1999) Diabetes mellitus and the risk of dementia: the Rotterdam Study. Neurology, 53: 1937–1942. [6] Sickmann HM, Waagepetersen HS, Schousboe A, Benie AJ, Bouman SD (2010) Obesity and type 2 diabetes in rats are associated with altered brain glycogen and amino-acid homeostasis. J Cereb Blood Flow Metab., 30:1527-1537. [7] Sinha S, Ekka M, Sharma UPR, Pandey RM, Jagannathan NR (2014) Assessment of changes in brain metabolites in Indian patients with type-2 diabetes mellitus using proton magnetic resonance spectroscopy. BMC Res Notes, doi: 10.1186/1756-0500-7-41

Current Grants

T. W. Scheenen, J. J. Fütterer, F. Witjes, M. Sedelaar, M. Maas, J. O. Barentsz, D. W. J. Klomp, H. H. Quick: Radboudumc: **A personalized image-based assessment of metastatic potential of prostate cancer** (2018-2021)

In this grant the assessment of the aggressiveness of localized prostate cancer is correlated and validated with early detection of the first metastases of the disease.

N. Axmacher, D. Timmann-Braun, H. H. Quick: DFG: **Focus group Neuroimaging: Extinction network connectivity across learning paradigms** (2017-2021)

In this joined project between PIs of the RUB and UKE, metaanalyses will be performed of fMRI data acquired in SFB1280. The main aim is to systematically investigate structural and functional extinction network connectivity across different learning paradigms and subject populations.

D. Timmann-Braun, H. H. Quick: DFG: **The contribution of the cerebellum to extinction: intrinsic mechanisms and cerebello-cerebral-interactions** (2017-2021)

The main aim of the project is to provide experimental evidence that the cerebellum has to be included as part of the neural circuitry underlying extinction of conditioned fear responses.

P. Koopmans: DFG Emmy Noether Programme – Independent Junior Research Group: **Functional Magnetic Resonance Imaging of cortical layers to measure directionality of information flow in brain networks for pain** (2016-2021)

Dr. Koopmans proposal focuses on the development of a high-resolution fMRI technique to improve understanding of how the brain processes pain.

T. W. Scheenen, H. H. Quick, J. O. Barentsz: Radboudumc: **Nanotechnology at ultra-high magnetic field: towards in vivo detection of small lymph node metastases with MRI** (2016–2020)

In this project the highest sensitivity of 7T to detect in vivo small lymph node metastases will be validated with histopathology of resected tissues in patients with rectal cancer.

M. E. Ladd, H.H. Quick, O. Speck: DFG: **German ultra-high field imaging (GUFI)**, Core Facility (2016-2019)

Aim of this project is to maintain and expand a nationwide network of UHF-MRI sites.

D. Timmann (PI), M. E. Ladd, A. Deistung (PI), J. Reichenbach: DFG: **In vivo assessment of the cerebellum by novel MRI techniques and application to hereditary ataxias: morphological, pathoanatomical and clinical aspects** (2015-2018)

The aim of this collaboration project is to obtain deeper insight into the pathoanatomy of cerebellar nuclei in common forms of degenerative ataxias by using novel MRI techniques.

H. H. Quick, D. G. Norris: **SIEMENS Healthcare GmbH: Cooperation agreement 7T High Field MR imaging, Erwin L. Hahn Institute** (2015-2018)

This cooperation agreement encompasses sequence and 7T MRI application development as well as ELH-provided feedback of clinical experience using the pTX Array step 2.

A. Rennings, K. Solbach, H. H. Quick: DFG: **Investigation of Electronic Band Gap (EBG) RF coils for 7T UHF-MRI** (2015-2017)

In this DFG-funded project, new transmit/receiver RF coils for UHF brain and body MRI using electronic band gap structures (EBG) are developed and evaluated.

M. Brand, K. Starcke: DFG: **Neural correlates of craving in patients with pathological buying – an fMRI study with a cue-reactivity paradigm** (2015-2017)

In the current project neural correlates of craving will be assessed in individuals with pathological buying with functional magnetic resonance imaging (fMRI).

D. Bodemer, M. Brand, N. Fuhr, M. Heisel, H. Hoppe, B. König, N. Krämer, S. Stieglitz, T. Zesch, J. Ziegler: **DFG Research Training Group: User-Centred Social Media** (2015-2017)

The Research Training Group addresses the need of analyzing, and understanding the characteristics and determinants of the behavior of Social Media users.

D. G. Norris, P. Hagoort: NWO: **Language regions in Interaction: An investigation of directional connectivity in the human language system using laminar fMRI** (2014-2018)

This ambitious project will examine the interaction between temporal cortex, and Broca's area during language comprehension using event-related fMRI at 7T.

B. Philips, T. W. Scheenen: Dutch Cancer Society: **Multi-parametric MRI of the prostate cancer: the next level** (2014-2017)

Multi-parametric MRI (mpMRI) of the prostate offers new possibilities for detection, localization and characterization of prostate cancer.

D. Norris, I. Tendolkar, M. Brand, J. Wiltfang, J. Schulz : Helmholtz-Gesellschaft: **Imaging and Curing Environmental Metabolic Diseases (ICEMED), Research Topic 4: Next generation CNS Imaging for metabolic disease** (2012-2018)

The primary goal of this project is to examine ways of improving cognitive deficits, particularly in episodic memory performance, in patients suffering from type 2 diabetes (T2DM).

M. E. Ladd, K. Solbach: European Research Council Advanced Grant: **MRexcite: Unlocking the potential of ultra-high field MRI through manipulation of radiofrequency excitation fields in human tissue** (2012-2017)

The goal of the project is to develop a highly optimized 32-channel transmit/receive RF coil for body MRI at 7T.

M. E. Ladd, H. H. Quick: Medical Faculty, University of Duisburg-Essen: **IFORES: Internal stipends for clinical researchers from University Hospital Essen** (2011-2017)

Various clinical researchers receive 12-months of intramural funding to conduct defined clinical research projects using 7T-MRI at the Erwin L. Hahn Institute.

Erwin L. Hahn Lecture 2017

Personnel and Organisational Structure at ELH

Directorate / Principal Investigators

Managing Director/PI
Prof. Dr. David G. Norris

Director/PI
Prof. Dr. Harald H. Quick
Prof. Dr. Matthias Brand

PI
Prof. Dr. Ulrike Bingel
Prof. Dr. Dagmar Timmann-Braun
Dr. Tom W. J. Scheenen
Prof. Dr. Mark E. Ladd
Dr. Peter J. Koopmans

Management

Administrative Director
Dr. Corinna Heldt
Judith Kösters

Staff Scientist
Dr. Oliver Kraff
Dr. Stefan Maderwald

Plug and Play-Scientist
Dr. Sören Johst

Radiographer
Lena Schäfer

Assistance
Sigrid Radermacher
Dirk Bremann

Public Relations
Stefanie Zurek

Scientists

MSc. Stephanie Antons
MSc. Jacob Bellmund
MSc. Sascha Brunheim
MSc. Guillermo Carbonell
Dr. med. Jens Claaßen
Dr. Andreas Deistung
Dr. med. Cornelius Deuschl
Dipl.-Phys. Thomas Ernst
Dr. med. Oliver Gembruch
Dr. rer. nat. Marcel Gratz
MSc. Donghyun Hong
Dr. Sören Johst
Dipl.-Phys. Fabian Kording
Dr. Christian Laier
MSc. Irati Markuerkiaga
Dr. Ivan Maximov
MSc. Silke M. Müller
Dipl.-Ing. Yacine Noureddine
Dr. Stephan Orzada
MSc. Viktor Pfaffenrot
MSc. Bart Philips
MSc. Stefan H. G. Rietsch
Dipl.-Psych. Christoph Ritter
MSc. Seyedmorteza Rohani Rankouhi
Dr. Astrid Rosenthal-von der Pütten
MSc. Katrin Scharmach
MSc. Jennifer Schulz
MSc. Daniel Sharoh
Dr. Katrin Starcke
Dr. med. Rutger Stijns
Prof. Dr. med. Indira Tendolkar
MSc. Jan-Willem Thielen
Dr. Patrick Trotzke
Dipl.-Ing. Maximilian Völker

Students

Luisa Bräuer
Jessica Gärtner
Viktor Pfaffenrot
Jonathan Weine

New in 2017

Raphaela Berghs
Jens Claaßen
Jessica Gärtner
Oliver Gembruch
Judith Kösters
Jessica Kohl
Peter Koopmans
Leonard Ruschen
Katharina Schröder
Nora Schulz
Jonathan Weine
Stefanie Zurek

Left in 2017

Raphaela Berghs
Luisa Bräuer
Dirk Bremann
Jessica Gärtner
Corinna Heldt
Sören Johst
Yacine Noureddine
Seyedmorteza Rohani Rankouhi
Leonard Ruschen
Jonathan Weine

Participation at ISMRM 2017 in Honolulu, Hawaii

Sascha Brunheim: Fast multi-slice B1 and B0 mapping (B01TIAMO) for 32-channel pTx body MRI at 7 Tesla
Marcel Gratz: On the Potential of DWI with Extrapolated High and Negative b-Values for Contrast Enhancement and Image Segmentation
Marcel Gratz: Impact of MR-based Motion Correction on clinical PET/MR data of patients with thoracic pathologies
Donghyun Hong: Regional GABA concentration comparison in the human brain with the interleaved short TE sLASER and MEGA-sLASER sequence at 7T
Donghyun Hong: Water lineshape fitting method to overcome B0 field inhomogeneity for NMR spectroscopy
Sören Johst: 32-Channel In-Vivo Parallel Transmit Body Imaging at 7 Tesla
Oliver Kraff: Safety and Function of Programmable Ventriculo-Peritoneal Shunt Valves: An in vitro 7 Tesla Magnetic Resonance Imaging Study
Oliver Kraff: RF safety of an implanted port catheter in direct vicinity of a 7T transmit head coil
Oliver Kraff: On the SAR load of typical head protocols at 7T
Mark Oehmigen: Impact of new attenuation correction methods on whole-body PET/MR
Stephan Orzada: A 32-channel transmit system add-on for 7 Tesla body imaging
Stephan Orzada: Transmit Arrays and Circuitry
Viktor Pfaffenrot: An 8/15-Channel Tx/Rx Head Neck RF Coil Combination with Semi-Dynamic B1 Shimming for Improved fMRI of the Cerebellum at 7T
Bart Philips: Initial Results of Combined 1H and 31P Spectroscopic Imaging of the Prostate at 7 Tesla
Stefan Rietsch: Initial tests of a 4-channel building block for a local 32-channel Rx-only body coil at 7T
Stefan Rietsch: Optimization of Remote RF Transmit Coil Elements and Arrays for 7T UHF Body MRI
Seyedmorteza Rohani Rankouhi: Editing of GABA at variable TEs with antiphase J-difference editing approach
Seyedmorteza Rohani Rankouhi: MASE-sLASER, a short TE matched chemical shift displacement error sequence for single voxel spectroscopy at ultrahigh field
Tom Scheenen: Prostate Cancer: Proton & Beyond
Tom Scheenen: USPIOs for Metastatic Lymph Node Detection in Prostate Cancer: Back on the Block
Nicolai Spicher: An open-source hardware and software system for video-gated MRI
Nicolai Spicher: On the importance of skin color phase variations for video measurement of cardiac activity in MRI
Maximilian Völker: Quality Assurance Phantoms and Procedures for UHF MRI—The German Ultrahigh Field Imaging (GUFI) Approach

Publications on 7T MRI

Beiderwellen, K.; Kraff, O.; Laader, A.; Maderwald, S.; Orzada, S.; Ladd, M.E.; Forsting, M.; Lauenstein, T.C.; Umutlu, L. (2017) Contrast enhanced renal MR angiography at 7 Tesla: How much gadolinium do we need? *European Journal of Radiology.* 86:76-82. doi: 10.1016/j.ejrad.2016.11.007 [Epub 2016 Nov 5.]

Brunheim, S.; Johst, S.; Pfaffenrot, V.; Maderwald, S.; Quick, H.H.; Poser, B.A. (2017) Variable slice thickness (VAST) EPI for the reduction of susceptibility artifacts in whole-brain GE-EPI at 7 Tesla. *Magnetic Resonance Materials in Physics, Biology and Medicine.* 30(2): 0968-5243. doi: 10.1007/s10334-017-0641-0

Brunheim, S; Gratz, M.; Johst, S.; Bitz, A.K.; Fiedler, T.M.; Ladd, M.E.; Quick, H.H.; Orzada, S. (2017) Fast and accurate multi-channel B1+ mapping based on the TIAMO technique for 7T UHF body MRI. *Magnetic Resonance in Medicine.* doi: 10.1002/mrm.26925 [Epub ahead of print]

Dammann, P; Wrede, K; Zhu, Y.; Matsushige, T.; Maderwald, S.; Umutlu, L.; Quick, H.H.; Hehr, U.; Rath, M.; Ladd, M.E.; Felbor, U.; Sure, U. (2017) Correlation of the venous angioarchitecture of multiple cerebral cavernous malformations with familial or sporadic disease: a susceptibility-weighted imaging study with 7-Tesla MRI. *Journal of Neurosurgery.* 126(2):570-577

Ernst, T.M.; Thürling, M.; Müller, S.; Kahl, F.; Maderwald, S.; Schlamann, M.; Boele, H.J.; Koekkoek, S.K.E.; Diedrichsen, J.; De Zeeuw, C.I.; Ladd, M.E.; Timmann, D. (2017) Modulation of 7 T fMRI Signal in the Cerebellar Cortex and Nuclei During Acquisition, Extinction, and Reacquisition of Conditioned Eyeblink Responses. *Human Brain Mapping.* 38(8):3957-3974. doi: 10.1002/hbm.23641 [Epub 2017 May 5.]

Fiedler, T.M.; Ladd, M.E.; Bitz, A.K. (2017) RF safety assessment of a bilateral four-channel transmit/receive 7 Tesla breast coil: SAR versus tissue temperature limits. *Medical Physics.* 44(1):143-157. doi: 10.1002/mp.12034.
Fiedler, T.M.; Ladd, M.E.; Bitz, A.K. (2017) Erratum: "RF safety assessment of a bilateral four-channel transmit/receive 7 Tesla breast coil: SAR versus tissue temperature limits" [*Medical Physics.* 44(1), 143-157 (2017)]. *Medical Physics.* 44(2):772. doi: 10.1002/mp.12145

Fiedler, T.M.; Ladd, M.E.; Bitz, A.K. (2017) SAR Simulations & Safety. *Neuroimage.* pii: S1053-8119(17)30243-4. doi: 10.1016/j.neuroimage.2017.03.035 [Epub ahead of print]

Fortuin, A.S.; Brüggemann, R.; van der Linden, J.; Panfilov, I.; Israël, B.; Scheenen, T.W.J.; Barentsz, J.O. (2017) Ultra-small superparamagnetic iron oxides for metastatic lymph node detection: back on the block. *Wiley Interdisciplinary Reviews: Nanomedicine and Nanobiotechnology.* 10(1). doi: 10.1002/wnan.1471 [Epub 2017 Apr 6. Review]

Gramsch, C.; Reuter, I.; Kraff, O.; Quick, H.H.; Tanislav, C.; Roessler, F.; Deuschl, C.; Forsting, M.; Schlamann, M. (2017) Nigrosome 1 visibility at susceptibility weighted 7T MRI-A dependable diagnostic marker for Parkinson's disease or merely an inconsistent, age-dependent imaging finding? *PLoS One.* 12(10):e0185489. doi: 10.1371/journal.pone.0185489

Kording, F; Ruprecht, C.; Schoennagel, B.; Fehrs, K.; Yamamura, J.; Adam, G.; Goebel, J.; Nassenstein, K.; Maderwald, S.; Quick, H.H.; Kraff, O. (2017) Doppler ultrasound triggering for cardiac MRI at 7T. *Magnetic Resonance in Medicine.* doi: 10.1002/mrm.27032 [Epub ahead of print]

Kraff, O.; Quick, H.H. (2017) 7T: Physics, safety, and potential clinical applications. *Journal of Magnetic Resonance Imaging.* doi: 10.1002/jmri.25723 [Epub ahead of print]

Laader, A.; Beiderwellen, K.; Kraff, O.; Maderwald, S.; Ladd, M.E.; Forsting, M.; Umutlu, L. (2017) Non-enhanced versus low-dose contrast-enhanced renal magnetic resonance angiography at 7 T: a feasibility study. *Acta Radiologica.* 1:284185117718399. doi: 10.1177/0284185117718399 [Epub ahead of print]

Laader, A.; Beiderwellen, K.; Kraff, O.; Maderwald, S.; Wrede, K.; Ladd, M.E.; Lauenstein, T.C.; Forsting, M.; Quick, H.H.; Nassenstein, K.; Umutlu, L. (2017) 1.5 versus 3 versus 7 Tesla in abdominal MRI: A comparative study. *PLoS One.* 10;12(11):e0187528. doi: 10.1371/journal.pone.0187528

Lagemaat, M.W.; Philips, B.W.; Vos, E.K.; van Uden, M.J.; Fütterer, J.J.; Jenniskens, S.F.; Scheenen, T.W.; Maas, M.C. (2017) Feasibility of Multiparametric Magnetic Resonance Imaging of the Prostate at 7 T. *Investigative Radiology.* 52(5):295-301. doi: 10.1097/RLI.0000000000000342

Marques, J.P.; Norris, D.G. (2017) How to choose the right MR sequence for your research question at 7T and above? *NeuroImage.* pii: S1053-8119(17)30341-5. doi: 10.1016/j.neuroimage.2017.04.044 [Epub ahead of print]

Noureddine, Y.; Kraff, O.; Ladd, M.E.; Wrede, K.H.; Chen, B.; Quick, H.H.; Schaefers, G.; Bitz, A.K. (2017) In vitro and in silico assessment of RF-induced heating around intracranial aneurysm clips at 7 Tesla. *Magnetic Resonance in Medicine.* doi: 10.1002/mrm.26650 [Epub ahead of print]

Orzada, S.; Ladd, M.E.; Bitz, A.K. (2017) A method to approximate maximum local SAR in multichannel transmit MR systems without transmit phase information. *Magnetic Resonance in Medicine.* 78(2), pp. 805-811. doi: 10.1002/mrm.26398

Orzada, S.; Bitz, A.K.; Johst, S.; Gratz, M.; Völker, M.N.; Kraff, O.; Abuelhaija, A.; Fiedler, T.M.; Solbach, K.; Quick, H.H.; Ladd, M.E. (2017) Analysis of an integrated 8-Channel Tx/Rx body array for use as a body coil in 7-Tesla MRI. *Frontiers in Physics.* Vol 5, id.17. doi: 10.3389/fphy.2017.00017

Philips, B.W.J.; Fortuin, A.S.; Orzada, S.; Scheenen, T.W.J.; Maas, M.C. (2017) High resolution MR imaging of pelvic lymph nodes at 7 Tesla. *Magnetic Resonance in Medicine.* 78(3):1020-1028. doi: 10.1002/mrm.26498 [Epub 2016 Oct 7.]

Rietsch, S.H.G; Pfaffenrot, V.; Bitz, A.K.; Orzada, S.; Brunheim, S.; Lazik-Palm, A.; Theysohn, J.M.; Ladd, M.E.; Quick, H.H.; Kraff, O. (2017) An 8-channel transceiver 7-channel receive RF coil setup for high SNR ultrahigh-field MRI of the shoulder at 7T. *Medical Physics.* 44(12):6195-6208. doi: 10.1002/mp.12612

Rietsch, S.H.; Orzada, S.; Bitz, A.K.; Gratz, M.; Ladd, M.E.; Quick, H.H. (2017) Parallel transmit capability of various RF transmit elements and arrays at 7T MRI. *Magnetic Resonance in Medicine.* doi: 10.1002/mrm.26704 [Epub ahead of print]

Wrede, K.H.; Matsushige, T.; Goericke, S.L.; Chen, B.; Umutlu, L.; Quick, H.H.; Ladd, M.E.; Johst, S.; Forsting, M.; Sure, U.; Schlamann, M. (2017) Non-enhanced magnetic resonance imaging of unruptured intracranial aneurysms at 7 Tesla: Comparison with digital subtraction angiography. *European Radiology.* (1):354-364 [Epub 2016 Mar 18.]

Awards

Prof. Dr. Matthias Brand, appointed co-editor at *Journal of Behavioral Addictions* and co-editor at *Sucht*

Sascha Brunheim, ISMRM Magna Cum Laude Merit Award for his contribution "Fast multi-slice B1 and B0 mapping (B01TIAMO) for 32-channel pTx body MRI at 7 Tesla"

Dr. Marcel Gratz, ISMRM Magna Cum Laude Award for his contribution "On the Potential of DWI with Extrapolated High and Negative b-Values for Contrast Enhancement and Image Segmentation"

Dr. Sören Johst, ISMRM Magna Cum Laude Merit Award for his contribution "32-channel in vivo parallel transmit body imaging at 7 Tesla"

Dr. Oliver Kraff, appointed Trainee Representative in the Governing Committee of the MR Safety Study Group, International Society for Magnetic Resonance in Medicine

Dr. Oliver Kraff, honored Distinguished Reviewer for *Magnetic Resonance in Medicine* during 2015-2016

Dr. Oliver Kraff, DAAD Travel Grant for participation at the 2017 ISMRM "Ensuring RF Safety in MRI" workshop, McLean, VA, USA

Prof. Dr. David G. Norris, appointed editor-in-chief at *MAGMA*

Dr. Stephan Orzada, ISMRM Magna Cum Laude Merit Award for his contribution „A 32-channel transmit system add-on for 7 Tesla body imaging"

Dr. Stephan Orzada, honored Distinguished Reviewer for *Magnetic Resonance in Medicine* during 2015-2016

Dr. Stephan Orzada, DAAD Travel Grant for participation at the 2017 ISMRM Joint Annual Meeting in Honolulu, HI, USA

Stefan H.G. Rietsch, DAAD Travel Grant for participation at the 2017 ISMRM Joint Annual Meeting in Honolulu, HI, USA

Tom W. J. Scheenen, ISMRM Outstanding Teacher Award for his contribution "Prostate Cancer: Proton & Beyond"

Nicolai Spicher, ISMRM Magna Cum Laude Award for his contribution "An open-source hardware and software system for video-gated MRI"

Dr. Oliver Gembruch and Dr. Jens Claaßen, awarded with a one-year IFORES-scholarship of the University Duisburg-Essen at the Erwin L. Hahn Institute

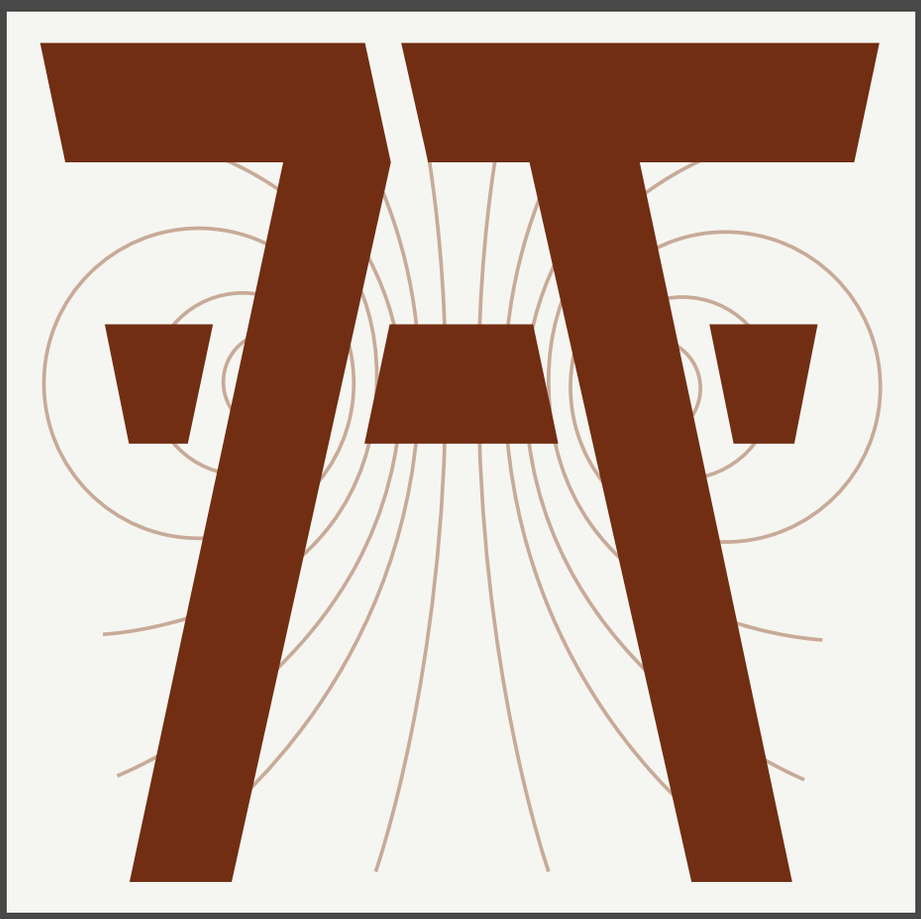

UNIVERSITÄT DUISBURG ESSEN
Open-Minded

UNIVERSITÄT DUISBURG ESSEN
INGENIEURWISSENSCHAFTEN

UMC St Radboud

Donders Institute
for Brain, Cognition and Behaviour

Universitätsklinikum Essen

Radboud Universiteit